



# Antarctic sea ice regime shift associated with decreasing zonal symmetry in the Southern Annular Mode

Serena Schroeter<sup>1</sup>, Terence J. O’Kane<sup>1,2</sup>, Paul A. Sandery<sup>1</sup>

<sup>1</sup>CSIRO Oceans and Atmosphere, Hobart, Tasmania, Australia

5 <sup>2</sup>Australian Centre for Excellence in Antarctic Science, Hobart, Tasmania, Australia

*Correspondence to:* Serena Schroeter (serena.schroeter@csiro.au)

**Abstract.** Across the long-term (~43 year) satellite record, Antarctic sea ice extent shows a small overall circumpolar increase, resulting from opposing regional sea ice concentration anomalies. Running short-term samples of the same sea ice concentration data, however, show that the long-term trend pattern is skewed towards the earliest years of the satellite record. 10 Compensating regional anomalies diminish over time, and in the most recent decade, these tend towards spatial homogeneity instead. Running 30-year trends show the regional pattern of sea ice behaviour reversing over time; while in some regions, trend patterns abruptly shift in line with the record anomalous sea ice behaviour of recent years, in other regions a steady change predates these record anomalies. The shifting regression patterns are co-located with enhanced north-south flow due to an increasingly wave-3-like structure of the Southern Annular Mode. Sea surface temperature anomalies also shift from a 15 circumpolar cooling to a regional pattern that resembles the increasingly asymmetric structure of the Southern Annular Mode, with warming in regions of previously increasing sea ice such as the Ross Sea.

## 1 Introduction

Contrary to expectations of sea ice coverage under a warming climate, sea ice in the Southern Ocean has not decreased over the satellite record as it has in the Arctic Ocean; rather, large diametrically opposed regional sea ice trends have resulted in a 20 small overall increase in Antarctic sea ice extent (Turner et al., 2015; Simmonds, 2015; Parkinson, 2019; Comiso et al., 2017). A small, steady increase in areal coverage between 1979-1999 was followed by an accelerated increase between 2000-2014 (Meehl et al., 2019), culminating in record high sea ice extent in 2014 (Comiso et al., 2017) before an unprecedentedly steep spring retreat in 2016 (Turner et al., 2017), and record low ice between 2017 and 2019 (Parkinson, 2019; Raphael and Handcock, 2022). While Antarctic sea ice returned to near average coverage in 2020, sea ice extent during the summer of 25 2021-22 reached the lowest point of the ~43-year satellite record (Raphael and Handcock, 2022; Wang et al., 2022). Sea ice is sensitive to changes in and interactions between the atmosphere and ocean (Hobbs et al., 2016), and indeed both atmospheric and oceanic influences have been identified to help explain the recent erratic behaviour (Turner et al., 2017; Stuecker et al., 2017; Wang et al., 2019; Schlosser et al., 2018; Meehl et al., 2019; Wang et al., 2022; Schossler et al., 2020). However, consensus is still lacking for not only the processes and mechanisms driving historical sea ice trends, but also the dominant 30 drivers of internal variability (Eayrs et al., 2019; Eayrs et al., 2021). Low confidence is currently placed in the simulation of mean and historical Antarctic sea ice in global coupled climate models, which tend not to accurately capture the spatial



heterogeneity or the seasonality of observed sea ice trends (Turner et al., 2013a; Hobbs et al., 2016; Eayrs et al., 2019). The disparity between simulated and observed sea ice is further complicated by the non-linearity of sea ice trends on both short-term and decadal scales (Handcock and Raphael, 2020; Eayrs et al., 2021). Additionally, the extent to which internal variability can account for the observed increase (as well as the disparity between observed and simulated trends) remains contested (Turner et al., 2013a; Mahlstein et al., 2013; Shu et al., 2015; Shu et al., 2020; Roach et al., 2020).

Recent examinations of Antarctic sea ice cover have generally considered the mean state and trends over the long-term, continuous satellite record (e.g. Eayrs et al., 2021; Raphael and Handcock, 2022; Parkinson, 2019). Climatological averaging smooths internal variability (which for Antarctic sea ice is known to be high), and is taken as reflective of the expected background state of Antarctic sea ice from which anomalies can be calculated. In a stationary or slowly-evolving variable, the climatological estimate can quite closely align with datapoints throughout the averaging period (Livezey et al., 2007). However, if significant trends exist in the averaging period, the background estimate may not be a realistic expectation from which future projections can be calculated (Arguez and Vose, 2011). It has long been noted that significant trends have existed during periods of the satellite record (Parkinson, 2019; Handcock and Raphael, 2020; Eayrs et al., 2021), which potentially shift the background estimate over time. Sea ice is strongly affected by atmospheric changes such as temperature, for which shorter 15-year temporal averages for climatological norms have been suggested (Arguez and Vose, 2011). Furthermore, while much of the literature reviewing Antarctic sea ice condenses metrics such as extent or areal cover into spatial averages or sums, either as a circumpolar total or a sector-based approach utilising geographical constraints (e.g. Zwally et al., 1983; Parkinson and Cavalieri, 2012; Parkinson, 2019) or spatial-autocorrelation dividing sea ice into regions of distinct interannual variability (e.g. Raphael and Hobbs, 2014), Antarctic sea ice trends are spatially heterogeneous, and large-scale averaging may neglect important small-scale regional trend characteristics.

This study presents a detailed examination of the temporal and spatial changes in Antarctic sea ice variability, comparing 15-year running samples of sea ice concentration with samples of large-scale atmospheric and oceanic variability patterns. Data and methods are described in Section 2, with results illustrated in Section 3. Discussion and concluding remarks are presented in Section 4.

## 2 Method

The monthly mean passive microwave satellite sea ice concentration data from the Climate Data Record are obtained from the National Snow and Ice Data Center (NSIDC), encompassing January 1979 – May 2021 (Meier et al., 2021b; Peng et al., 2013). This timeseries is then supplemented with monthly averages of the daily near-real-time Climate Data Record (Meier et al., 2021a) for June – December 2021. Satellite data is obtained on the native equal-area 25km polar stereographic grid (<https://nsidc.org/data/ease>). In order to obtain estimates of sea ice area and extent at each longitude point, the sea ice concentration (SIC) data are reprojected and regridded onto a regular 1° latitude x 1° longitude grid. Following convention, at each longitude, sea ice extent (SIE) is calculated as the sum of the product of grid cell area for cells with at least 15% ice



65 coverage, and sea ice area (SIA) is calculated as the sum of the product of grid cell area and ice area fraction (e.g. Roach et al., 2020).

Monthly averaged mean sea level pressure (SLP) between January 1979 – December 2021 from the Japanese Meteorological Agency (JMA) global atmospheric reanalysis JRA-55 (Kobayashi et al. 2015) are obtained from the Research Data Archive at the National Center for Atmospheric Research, Computational and Information Systems Laboratory (<https://doi.org/10.5065/D60G3H5B>). Sea surface temperature (SST) data is obtained from the Met Office Hadley Centre  
70 (<https://www.metoffice.gov.uk/hadobs/hadisst/>) Sea Ice and Sea Surface Temperature dataset version 2 (HadISST.2.2.0.0, hereafter HadISST2 (Titchner and Rayner, 2014)). HadISST2 is provided by the Met Office on a 1° latitude by 1° longitude grid; the 1.25° JRA-55 data is regridded onto the same grid for consistency in comparing with SIC and SST.

To prepare data for analysis, each dataset is sliced into running 15-year (e.g. January 1979-December 1993, January 1980-December 1994 etc.) or 30-year samples depending on the context, from which climatological means and anomalies are  
75 calculated. Empirical orthogonal analysis (EOF) patterns are calculated from the 15-year samples following detrending and weighting by cosine of latitude, to compensate for the convergence of meridians near the pole.

### 3 Results

The large annual cycle of Antarctic sea ice (Figure 1a) has shifted over time, with running 15-year monthly average sea ice extent (SIE) and area (SIA) deviations from the 1979-2021 mean clearly showing a steady increase over the satellite record  
80 that reverses in the most recent samples (Figure 1b-c). Given the anomalously low sea ice occurring between 2016-2021 (described in Section 1), these shorter-than-typical climatologies merely highlight the nullifying impact of recent record low sea ice events. However, the proportion of 15-year samples exceeding the 1979-2021 mean is greater than half year-round, indicating that despite recent record low sea ice, the long-term mean of both SIA and SIE is skewed towards the earliest years. The skewness is particularly high during late summer and autumn (e.g. 22 of 29 SIA samples above the 1979-2021 mean in  
85 April-May and December), which is also when the largest sea ice trends have been observed (Hobbs et al., 2016; Holland, 2014; Eayrs et al., 2019). Calculating anomalies from a biased long-term sea ice average may obscure or misrepresent variability at short-term timescales, hindering robust interpretation of sea ice behaviour and trends. We posit that the magnitude or even sign of observed anomalous sea ice behaviour changes substantially under different timespans: for example, if sea ice anomalies were calculated from a sample encompassing only the most recent decades, the short-term climatologies imply that  
90 the negative anomalies since 2016 would appear even more extreme, as mean sea ice is of a higher magnitude than the mean of the ~43 year climatology.

Spatially, the increasing mean SIE and SIA described above is most notable from west of the Dumont D'Urville Sea to the Ross Sea, as well as in the Haakon VII Sea, while mean sea ice steadily decreases in the Bellingshausen and western Weddell seas (Figure 1d-e). Compensating anomalies and opposing trends have long been noted in the aforementioned regions  
95 (Parkinson, 2019; Parkinson and Cavalieri, 2012; Comiso et al., 2017; Turner et al., 2015; Simmonds, 2015). The negative



regional anomalies reduce the magnitude of the positive regional anomalies to produce a smaller circumpolar value that has increased fairly steadily over time until 2016, with a positive regression line of 7304.97 km<sup>2</sup> per year for SIE and 6976.73 km<sup>2</sup> per year for SIA between 1979 and 2021 (Figure 2a).

100 However, a simple linear regression of annual circumpolar SIE and SIA anomalies for only the most recent 30 years (1992-2021) produces negative trendlines, of -4345 km<sup>2</sup> per year for SIE and -3513.31 km<sup>2</sup> for SIA (Figure 2a). Furthermore, a standard deviation of annual SIE and SIA anomalies reveals a decrease in regional variability over time (Figure 2b). Contours of annual SIA anomalies by region (Figure 2c; SIA is presented instead of SIE as it is less noisy, though both show the same decreasing variability pattern) indeed show that strongly opposing regional anomalies tended to occur earlier in the satellite record (e.g. 1980, 1992 and 1998-2000). In much of the most recent decade, however, anomalies have veered toward the same  
105 sign in those regions, so despite the anomalies tending to be lower magnitude than in earlier years, the compounding effect of spatially-homogeneous anomalies rather than spatially-compensating anomalies leads to higher-magnitude annual average anomalies overall.

Eigenvectors produced through empirical orthogonal analysis (EOFs; also known as principal component analysis) show the spatial pattern that accounts for the maximum proportion of variance in a dataset. The first (highest-variance-explained) EOF  
110 pattern for the earliest sample (1979-1993) of sea ice concentration (SIC) shows a pattern of strongly opposing anomalies between the Bellingshausen, Weddell and far western Ross seas and the Ross, Amundsen and Haakon VII seas, concentrated at the ice edge (Figure 3a). In the most recent SIC sample (2007-2021), however, the strength of the opposing anomalies is much diminished, and the anomalies in the Amundsen and Bellingshausen seas are shifted eastward (Figure 3b). The anomalies are also spread further throughout the sea ice zone rather than the ice edge. As the sign of anomalies is fairly consistent at each  
115 longitude, averaging EOF1 at each longitude for the 15-year samples emphasises the diminution through time of opposing anomalies between the Ross/Amundsen seas and Bellingshausen Sea (Figure 3d). Pattern correlations of EOF1 for running 15-year SIC samples with Figure 3a and Figure 3b highlight that the change in the pattern of maximum SIC variance has been steady over time (Figure 3c).

120 Despite statistically significant (albeit low-magnitude) positive trends in Antarctic sea ice existing over the satellite record, strong non-linearity occurs within the trend due to high decadal and sub-decadal variability (Handcock and Raphael, 2020). Contrary to the small increasing 42-year trend, a least-squares linear regression line for only the most recent 30-year period (1992-2021) produces a small decrease in SIA and SIE (Figure 2b). Calculating running regression lines of anomalies from 30-year samples (15-year samples tending to be too noisy due to high internal variability) reveals a very different picture than the long-term trend implies (Figure 4). The “compensating” regional dipole of anomalies (positive in the Ross, Weddell and  
125 western Haakon VII seas and negative in the Amundsen and Bellingshausen seas (Parkinson, 2019; Parkinson and Cavalieri, 2012; Comiso et al., 2017; Turner et al., 2015; Simmonds, 2015) ) is substantially dampened over time. In the most recent regression pattern, the sign of the long-term trend pattern is almost reversed, with decreasing SIA in the Ross Sea and most of the Weddell Sea, increasing SIA in the Amundsen and western Weddell seas, and close to zero SIA trend in the Bellingshausen and Haakon VII seas.



130 Diminishing regression coefficients in the Amundsen, Bellingshausen and western Weddell Sea are consistent through time, clearly pre-dating the recent anomalously low-sea ice years. In contrast, changing patterns in the Ross, eastern Weddell and Haakon VII seas are noisy in the earliest samples but abruptly shift in samples that coincide with the anomalously sharp sea ice retreat in 2016 and beyond, which has been attributed to unusual atmospheric and oceanic conditions in the Southern Ocean (Turner et al., 2017; Stuecker et al., 2017; Wang et al., 2019; Schlosser et al., 2018; Meehl et al., 2019).

### 135 **3.1 Meridional structure shift in the Southern Annular Mode**

Interannual variability and trends in Antarctic sea ice are strongly influenced by wind, through both thermodynamic and dynamic effects (e.g. Hobbs et al., 2016; Raphael and Hobbs, 2014; Schroeter et al., 2017; Matear et al., 2015; Holland and Kwok, 2012; Haumann et al., 2014; Hall and Visbeck, 2002; Bernades Pezza et al., 2012; Stammerjohn et al., 2008). Atmospheric circulation in the Southern Hemisphere high latitudes is predominantly zonally-symmetric, with a strong westerly polar jet encircling the continent near 60°S (Kidson and Sinclair, 1995). The dominant mode of Southern Hemisphere atmospheric variability, the Southern Annular Mode (SAM), is often described as a predominantly annular (ring-like) structure of opposing anomalies between the mid- and high-latitudes (Gong and Wang, 1999; Thompson and Wallace, 2000; Marshall, 2003). However, there are mechanisms of asymmetric flow embedded within the otherwise zonal atmospheric circulation, such as poleward propagating Rossby wave trains from the tropics known as the Pacific South-American (PSA) modes (Mo and Higgins, 1998; Mo and Paegle, 2001), and the quasi-stationary zonal waves 1 and 3 (ZW3) (Hobbs and Raphael, 2010; Raphael, 2004). A zonal wave-3 pattern is embedded with the SAM itself, with a ring-like pattern of anomalies containing three non-annular components can be clearly seen around Antarctica, juxtaposed with three non-annular components in the belt of opposing mid-latitude anomalies (Figure 5a). Trends calculated since 1979 show SAM tending towards its positive phase (Fogt and Marshall, 2020). During the positive SAM phase, negative pressure anomalies occur over the Antarctic region, projecting onto the climatological low-pressure centre in the Amundsen Sea (the Amundsen Sea Low (Fogt et al., 2012b; Raphael et al., 2015; Turner et al., 2013b)), resulting in enhanced local meridional winds and disparate regional sea ice behaviour in the Ross, Amundsen, Bellingshausen and Weddell seas (Holland et al., 2017). Positive SAM is also associated with a strengthening of the westerly polar jet, which is evident in 15-year running samples of 850hPa zonal winds (see Figure S1). An increasingly annular pattern of atmospheric flow implies stronger zonal winds over the sea ice zone (outside the ASL region), and would tend to produce more northward sea ice transport through the Ekman effect (Hall and Visbeck, 2002). However, though the structure of SAM shows seasonal and decadal variability (Fogt et al., 2012a), in recent years the structure of the SAM has become increasingly asymmetric (Wachter et al., 2020; Campitelli et al., 2022), indicating more north-south airflow around the continent and, as a result, more spatially heterogeneous sea ice behaviour. In EOF1 of SLP between 1979 and 1993 (Figure 5b), the structure of SAM closely reflects the long-term mean (Figure 5a). However, in more recent 15-year samples (e.g. 2007-2021; Figure 5c) the annular structure becomes more wave-like, as the non-annular components in the mid-latitudes contract southwards.



The difference between early samples and more recent samples (Figure 5d) essentially reproduces the pattern of the asymmetric SAM component at 700hPa (Campitelli et al., 2022), and zonal SAM anomalies averaged between  $-70^{\circ}\text{S}$  and  $-55^{\circ}\text{S}$  (Figure 5d) show a consistent shift in structure from annular to increasingly wave-3-like. The deepening and longitudinal contraction of the non-annular component in the Amundsen Sea positions it further away from the Ross Sea, with a clear reduction in cyclonic flow over the west of this region (Figure 5c). As discussed previously, the sign of sea ice anomalies in the Ross, Amundsen and Bellingshausen seas has essentially reversed throughout the samples (Figure 4). These regions of sea ice change are co-located with the shift towards asymmetric SAM, as shown by the gradient of zonal SAM anomalies over the samples (Figure 6). Though the increasing asymmetry of SAM is also evident between the Haakon VII and Dumont D'Urville seas, sea ice anomalies in these regions (which are dominated by cyclonic activity rather than large-scale atmospheric modes (Matear et al., 2015; Schroeter et al., 2017; Turner et al., 2015)) show no clear corresponding response. The Weddell Sea is situated in between the increasing anticyclonic flow directly to the north and cyclonic circulation to the west of the Antarctic Peninsula (Figure 5b and c), implying enhanced northerly flow over the region. The increasingly positive SIA anomalies in the western Weddell Sea and the precipitous drop in anomalies to the central and east are in agreement with the dynamic and thermodynamic effects of increased northerly winds, i.e. reducing extent by pushing sea ice poleward, increased convergence of sea ice along the western coastline, and warmer surface temperatures enhancing melt and impeding ice production.

### 3.2 Changes in Southern Ocean Sea Surface Temperature

Climatological reconstructions suggest that sea surface temperature (SST) across the Southern Ocean increased across much of the early- and mid-20<sup>th</sup> century before exhibiting a reversal in the late 1970s (Turney et al., 2017). In the decades following, a regime shift occurs, towards a “warm state” in which the Indian Ocean and western boundary currents of the Southern Ocean warm but the high-latitude SSTs cool (Freitas et al., 2015). In line with the increase in mean Antarctic sea ice since 1979, high-latitude SSTs in the Southern Ocean have decreased, associated with strengthening westerly winds and negative pressure anomalies (Fan et al., 2014; Armour et al., 2016; Blanchard-Wrigglesworth et al., 2021). The shift to positive SAM is also associated with thermodynamic atmospheric changes, such as enhanced cooling and drying of the atmosphere overlying the high-latitude Southern Ocean, and reduced downwelling longwave radiation, which lead to negative SST anomalies (Kusahara et al., 2017; Doddridge and Marshall, 2017). A nonmonotonic, two-timescale Southern Ocean SST response to SAM is seen in many global coupled climate models, in which abrupt SST cooling through anomalous equatorward Ekman drift occurs under a transition to positive SAM, but gradually reverts towards a warming signal due to either advective or mixing-based mechanisms over the longer-term (Kostov et al., 2017; Ferreira et al., 2015; Seviour et al., 2019; Doddridge et al., 2021). However, a warming SST signal has eluded the observational record thus far, with mechanisms such as eddy compensation potentially dampening the effect of wind-driven upwelling (Doddridge et al., 2019). Nonetheless, recent work shows that observed sea ice trend patterns cannot be explained by winds alone, requiring nudging of SST north of the sea ice edge towards observations in order to reproduce observed trends (Blanchard-Wrigglesworth et al., 2021). Given the close association of SST



195 in the region north of the sea ice edge to both sea ice anomalies and SAM, and the shifting patterns of both (Figures 4 and 5),  
we now examine running anomalies of SST.

Although the long-term (1979-2021) trend of sea surface temperature (SST) within the sea ice zone and just north of the sea  
ice edge is negative, mid-latitude SSTs are increasing (Figure 7a). Considering the regression coefficients of only the most  
recent 30-year period (1992-2021), the trend pattern is less widespread around the western Ross Sea, but more so in the  
Amundsen and Bellingshausen seas (Figure 7b). Over the last 15 years (2007-2021), however, a wave-3-like pattern of SST  
200 anomalies appears instead (Figure 7c), bearing resemblance to the enhanced meridional pattern of SAM (Figure 5b).

Regression coefficients of 30-year samples of SST anomalies north of the ice edge (-55°S to -40°S) show a reversal of the  
dipole between the region above the western and eastern Ross Sea; whereas in early 30-year samples the region north of the  
western Ross Sea was clearly cooling compared to warming to the east, SSTs are increasing across the region in the most  
recent sample (Figure 7d). SSTs are also increasing north of the Bellingshausen Sea, but declining sharply in recent samples  
205 across the neighbouring region above the Amundsen Sea. North of the Weddell Sea, 30-year trends of SSTs above the sea ice  
zone are decreasing to the west and showing little clear tendency above the central Weddell Sea. Only in the far east, adjacent  
to Haakon VII Sea, do SST trends show an increasing tendency before dropping again in line with enhanced southerly flow  
under the increased asymmetry of SAM.

#### 4 Discussion and Conclusions

210 We use short-term running means and anomalies to show that, while climatological Antarctic sea ice has increased over the  
satellite record, the long-term pattern is skewed towards the earliest years, and is reversing across much of the sea ice zone,  
particularly in the Haakon VII, Ross and Bellingshausen seas. The long-term trend of circumpolar sea ice anomalies shows a  
small expansion over time, which has long been cited as the result of high-magnitude opposing regional anomalies; however,  
the regional sea ice dipole decreases over the past decade, with smaller but more spatially homogeneous compounding  
215 anomalies. Trends of anomalies based on running 30-year samples reveal a reversal of both the increasing trend in the Ross,  
Weddell and Haakon VII seas and the decreasing trend in the Amundsen and Bellingshausen seas. Indeed, the most recent 30-  
year sample shows negative trends in the Ross and eastern Weddell seas, positive trends in the Amundsen and western Weddell  
seas, and close to zero trend in the Bellingshausen Sea. Though some of these trend patterns shift more abruptly due to the  
recent anomalous sea ice declines, the reversal in other regions has been consistent across the samples.

220 It is clear that the long-term circumpolar sea ice increase has been abruptly interrupted by the record low sea ice between 2016-  
2019, with the rate of decline over those few years equalling the rate of decline over 30 years in the Arctic (Handcock and  
Raphael, 2020; Parkinson, 2019; Eayrs et al., 2021). However, several studies using ice cores and whaling records also  
identified sharp sea ice declines in the decades preceding the satellite sea ice record, particularly in the late 1970s just prior to  
the launch of the satellite record that also was sharpest in the Weddell Sea (Kukla and Gavin, 1981; De La Mare, 1997; Curran  
225 et al., 2003; De La Mare, 2009; Cotte and Guinet, 2007). Simulations investigating multi-decadal sea ice trends which



reproduced the small overall increase in Antarctic sea ice also produced decreasing sea ice in the decades prior to the satellite record (Goosse et al., 2009). That these declines were then followed by the observed overall increase for several decades raises speculation as to whether Antarctic sea ice is simply very responsive to sharp changes in atmospheric or oceanic conditions, and is capable of recovering from those declines over the ensuing decades (Parkinson, 2019; Eayrs et al., 2021).

230 As the dominant mode of large-scale atmospheric circulation in the Southern Hemisphere, SAM has a strong impact on sea ice, particularly in the West Antarctic region (Lefebvre and Goosse, 2005; Lefebvre et al., 2004; Holland et al., 2017; Doddridge and Marshall, 2017; Stammerjohn et al., 2008; Schroeter et al., 2017; Raphael and Hobbs, 2014; O’kane et al., 2013b). Several studies have noted that, prior to 1978, Southern Hemisphere mid-latitude circulation was dominated by a metastable blocking regime, in which zonally symmetric circulation is suppressed in favour of heightened meridional motion

235 (O’kane et al., 2013a; Freitas et al., 2015). Following the late 1970s, however, a regime shift occurred in which SAM (which was previously associated with a transition state) replaced the negative phase of this blocking pattern, increasing zonally-symmetric (annular) circulation in both frequency and intensity and reducing the occurrence and persistence of blocking (O’kane et al., 2013a; Freitas et al., 2015; Franzke et al., 2015). Surface air temperatures and Southern Ocean SSTs reflected the weakened blocking state (Freitas et al., 2015; O’kane et al., 2013b; Franzke et al., 2015), and the strength of the subtropical

240 jet decreased while upper tropospheric zonal wind strength increased north of the sea ice zone (Frederiksen et al., 2011; Frederiksen and Frederiksen, 2007). However, as SAM has a zonal wave-3 structure embedded within it, the intensifying annular mode has in recent years undergone a shift towards its asymmetric component (Wachter et al., 2020; Campitelli et al., 2022), increasing meridional flow over the sea ice zone and driving spatially heterogeneous anomalies. This may at first appear counterintuitive, as our analysis shows that recent sea ice anomalies are in greater agreement across the regions of high-

245 magnitude change; however, we also show that the structural shift in SAM is co-located with changing Antarctic sea ice anomalies and reversing trends, implying that a sea ice response to north-south wind changes is already underway and likely to continue in line with an intensifying asymmetric flow pattern. Though rebounding of sea ice has followed sharp declines in the past, an increase in the occurrence and intensity of the positive phase of SAM leads to increased temperatures in the subsurface ocean, as well as increased upwelling close to the continent (Verfaillie et al., 2022), with substantial implications

250 for sea ice as vertical heat transport and storage preconditions sea ice for rapid retreat in coming seasons (Doddridge et al., 2021). Our results also show that Southern Ocean SSTs are shifting, away from circumpolar cooling in the sea ice zone towards an intensified regional pattern. Compared with earlier decades of the satellite record, the SST anomaly pattern north of the sea ice zone in recent years also alludes to the wave-3 pattern of the asymmetric SAM structure; if both the wave-3 SST pattern and warmer SSTs persist, a rapid sea ice recovery in coming years is unlikely.

255





### Code and data availability

The NSIDC monthly mean passive microwave satellite sea ice concentration Climate Data Record is available at <https://nsidc.org/data/G02202>. The daily near-real-time Climate Data Record is available at <https://nsidc.org/data/g10016>. The Japanese Meteorological Agency (JMA) global atmospheric reanalysis JRA-55 is available at <https://doi.org/10.5065/D60G3H5B>. The Met Office Hadley Centre Sea Ice and Sea Surface Temperature dataset version 2 (HadISST.2.2.0.0) is available at <https://www.metoffice.gov.uk/hadobs/hadisst/>.

### Author contribution

SS designed the study, performed the analysis, created the plots and drafted the manuscript. TO and PS provided important guidance, and all authors discussed and revised the manuscript.

### Competing interests

The authors declare that they have no conflict of interest.

### Acknowledgements

Serena Schroeter was supported by a CSIRO Early Research Career Fellowship. This research/project was undertaken with the assistance of resources and services from the National Computational Infrastructure (NCI), which is supported by the Australian Government.

### References

- Arguez, A. and Vose, R. S.: The definition of the standard WMO climate normal: The key to deriving alternative climate normals, *Bulletin of the American Meteorological Society*, 92, 699-704, 2011.
- Armour, K. C., Marshall, J., Scott, J. R., Donohoe, A., and Newsom, E. R.: Southern Ocean warming delayed by circumpolar upwelling and equatorward transport, *Nature Geoscience*, 2016.
- Bernades Pezza, A., Rashid, H. A., and Simmonds, I.: Climate links and recent extremes in Antarctic sea ice, high-latitude cyclones, Southern Annular Mode and ENSO, *Climate dynamics*, 38, 57-73, 2012.
- Blanchard-Wrigglesworth, E., Roach, L. A., Donohoe, A., and Ding, Q.: Impact of winds and Southern Ocean SSTs on Antarctic sea ice trends and variability, *Journal of Climate*, 34, 949-965, 2021.
- Campitelli, E., Diaz, L. B., and Vera, C.: Assessment of zonally symmetric and asymmetric components of the Southern Annular Mode using a novel approach, *Climate Dynamics*, 58, 161-178, 2022.
- Comiso, J. C., Gersten, R. A., Stock, L. V., Turner, J., Perez, G. J., and Cho, K.: Positive trend in the Antarctic sea ice cover and associated changes in surface temperature, *Journal of Climate*, 30, 2251-2267, 2017.
- Cotte, C. and Guinet, C.: Historical whaling records reveal major regional retreat of Antarctic sea ice, *Deep Sea Research Part I: Oceanographic Research Papers*, 54, 243-252, 2007.
- Curran, M. A., van Ommen, T. D., Morgan, V. I., Phillips, K. L., and Palmer, A. S.: Ice core evidence for Antarctic sea ice decline since the 1950s, *Science*, 302, 1203-1206, 2003.



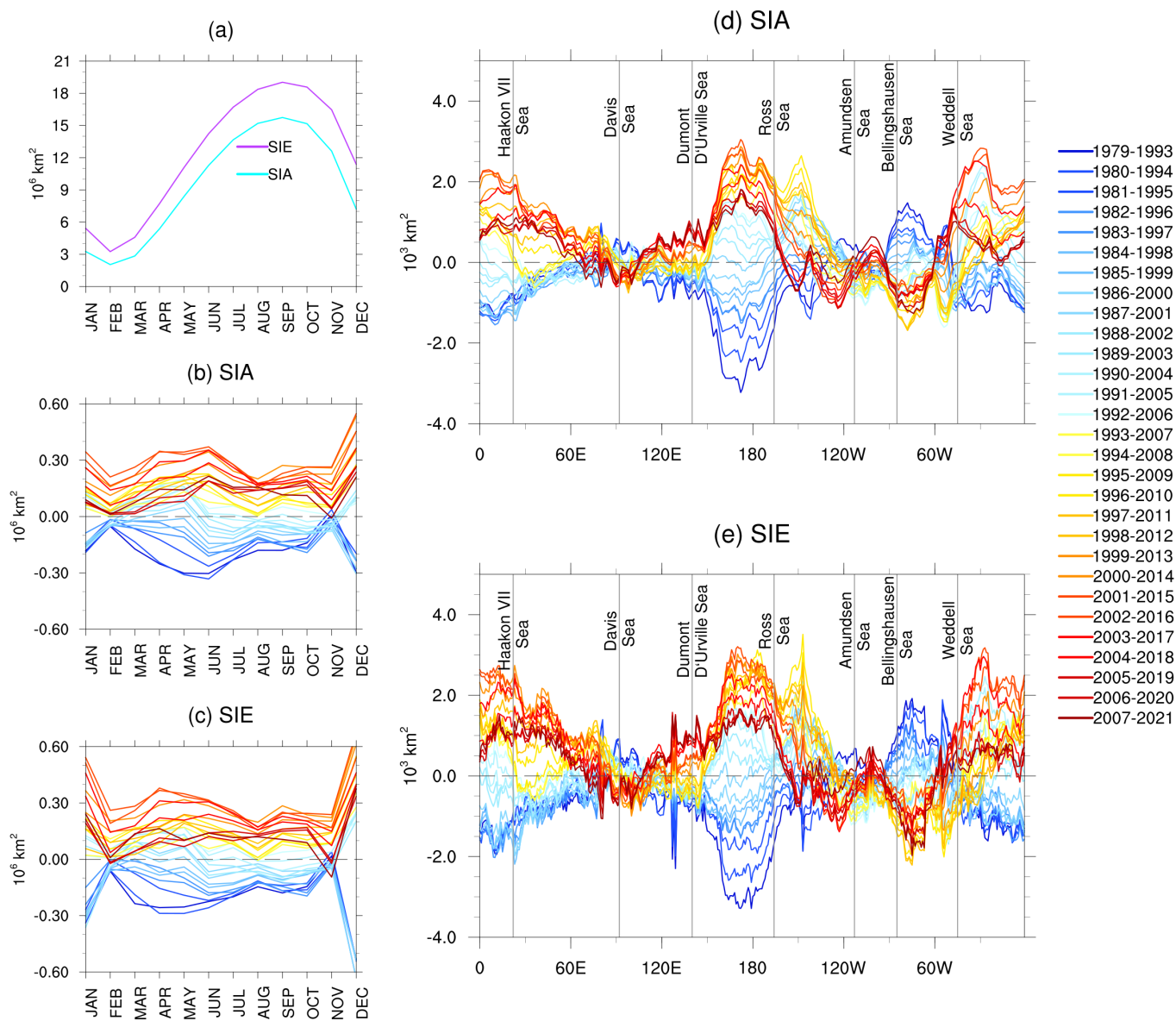
- 290 de la Mare, W. K.: Abrupt mid-twentieth-century decline in Antarctic sea-ice extent from whaling records, *Nature*, 389, 57-60, 10.1038/37956, 1997.
- de la Mare, W. K.: Changes in Antarctic sea-ice extent from direct historical observations and whaling records, *Climatic Change*, 92, 461-493, 10.1007/s10584-008-9473-2, 2009.
- 295 Doddridge, E. W. and Marshall, J.: Modulation of the Seasonal Cycle of Antarctic Sea Ice Extent Related to the Southern Annular Mode, *Geophysical Research Letters*, 44, 9761-9768, <https://doi.org/10.1002/2017GL074319>, 2017.
- Doddridge, E. W., Marshall, J., Song, H., Campin, J.-M., and Kelley, M.: Southern Ocean heat storage, reemergence, and winter sea ice decline induced by summertime winds, *Journal of Climate*, 34, 1403-1415, 2021.
- Doddridge, E. W., Marshall, J., Song, H., Campin, J. M., Kelley, M., and Nazarenko, L.: Eddy compensation dampens Southern Ocean sea surface temperature response to westerly wind trends, *Geophysical Research Letters*, 46, 4365-4377, 2019.
- 300 Eayrs, C., Li, X., Raphael, M. N., and Holland, D. M.: Rapid decline in Antarctic sea ice in recent years hints at future change, *Nature Geoscience*, 1-5, 2021.
- Eayrs, C., Holland, D., Francis, D., Wagner, T., Kumar, R., and Li, X.: Understanding the Seasonal Cycle of Antarctic Sea Ice Extent in the Context of Longer-Term Variability, *Reviews of Geophysics*, 57, 1037-1064, 2019.
- Fan, T., Deser, C., and Schneider, D. P.: Recent Antarctic sea ice trends in the context of Southern Ocean surface climate variations since 1950, *Geophysical Research Letters*, 41, 2419-2426, 10.1002/2014GL059239, 2014.
- 305 Ferreira, D., Marshall, J., Bitz, C. M., Solomon, S., and Plumb, A.: Antarctic ocean and sea ice response to ozone depletion: A two-time-scale problem, *Journal of Climate*, 28, 1206-1226, 10.1175/JCLI-D-14-00313.1, 2015.
- Fogt, R. L. and Marshall, G. J.: The Southern Annular Mode: variability, trends, and climate impacts across the Southern Hemisphere, *Wiley Interdisciplinary Reviews: Climate Change*, 11, e652, 2020.
- 310 Fogt, R. L., Jones, J. M., and Renwick, J.: Seasonal zonal asymmetries in the Southern Annular Mode and their impact on regional temperature anomalies, *Journal of Climate*, 25, 6253-6270, 2012a.
- Fogt, R. L., Wovrosh, A. J., Langen, R. A., and Simmonds, I.: The characteristic variability and connection to the underlying synoptic activity of the Amundsen-Bellinghousen Seas Low, *Journal of Geophysical Research: Atmospheres*, 117, 10.1029/2011JD017337, 2012b.
- 315 Franzke, C., O'Kane, T., Monselesan, D., Risbey, J., and Horenko, I.: Systematic attribution of observed Southern Hemisphere circulation trends to external forcing and internal variability, *Nonlinear Processes in Geophysics*, 22, 513-525, 2015.
- Frederiksen, J., Frederiksen, C., Osbrough, S., and Sisson, J. M.: Changes in Southern Hemisphere rainfall, circulation and weather systems, 19th International Congress on Modelling and Simulation, 2712-2718,
- Frederiksen, J. S. and Frederiksen, C. S.: Interdecadal changes in southern hemisphere winter storm track modes, *Tellus A: Dynamic Meteorology and Oceanography*, 59, 599-617, 2007.
- 320 Freitas, A. C., Frederiksen, J. S., Whelan, J., O'Kane, T. J., and Ambrizzi, T.: Observed and simulated inter-decadal changes in the structure of Southern Hemisphere large-scale circulation, *Climate Dynamics*, 45, 2993-3017, 2015.
- Gong, D. and Wang, S.: Definition of Antarctic oscillation index, *Geophysical Research Letters*, 26, 459-462, 1999.
- Goosse, H., Lefebvre, W., de Montety, A., Cresspin, E., and Orsi, A. H.: Consistent past half-century trends in the atmosphere, the sea ice and the ocean at high southern latitudes, *Climate Dynamics*, 33, 999-1016, 2009.
- 325 Hall, A. and Visbeck, M.: Synchronous Variability in the Southern Hemisphere Atmosphere, Sea Ice, and Ocean Resulting from the Annular Mode, *Journal of Climate*, 15, 3043-3057, 2002.
- Handcock, M. S. and Raphael, M. N.: Modeling the annual cycle of daily Antarctic sea ice extent, *The Cryosphere*, 14, 2159-2172, 2020.
- Haumann, F. A., Notz, D., and Schmidt, H.: Anthropogenic influence on recent circulation-driven Antarctic sea ice changes, *Geophysical Research Letters*, 41, 8429-8437, 10.1002/2014GL061659, 2014.
- 330 Hobbs, W. R. and Raphael, M. N.: Characterizing the zonally asymmetric component of the SH circulation, *Climate Dynamics*, 35, 859-873, 2010.
- Hobbs, W. R., Massom, R., Stammerjohn, S., Reid, P., Williams, G., and Meier, W.: A review of recent changes in Southern Ocean sea ice, their drivers and forcings, *Global and Planetary Change*, 143, 228-250, 10.1016/j.gloplacha.2016.06.008, 2016.
- Holland, M. M., Landrum, L., Kostov, Y., and Marshall, J.: Sensitivity of Antarctic sea ice to the Southern Annular Mode in coupled climate models, *Climate Dynamics*, 49, 1813-1831, 2017.
- 335 Holland, P. R.: The seasonality of Antarctic sea ice trends, *Geophysical Research Letters*, 41, 4230-4237, 10.1002/2014GL060172, 2014.
- Holland, P. R. and Kwok, R.: Wind-driven trends in Antarctic sea-ice drift, *Nature Geoscience*, 5, 872-875, 10.1038/ngeo1627, 2012.
- Kidson, J. W. and Sinclair, M. R.: The influence of persistent anomalies on Southern Hemisphere storm tracks, *Journal of climate*, 8, 1938-1950, 1995.
- 340 Kostov, Y., Marshall, J., Hausmann, U., Armour, K. C., Ferreira, D., and Holland, M. M.: Fast and slow responses of Southern Ocean sea surface temperature to SAM in coupled climate models, *Climate Dynamics*, 48, 1595-1609, 2017.
- Kukla, G. and Gavin, J.: Summer ice and carbon dioxide, *Science*, 214, 497-503, 1981.
- Kusahara, K., Williams, G. D., Massom, R., Reid, P., and Hasumi, H.: Roles of wind stress and thermodynamic forcing in recent trends in Antarctic sea ice and Southern Ocean SST: An ocean-sea ice model study, *Global and Planetary Change*, 158, 103-118,
- 345 10.1016/j.gloplacha.2017.09.012, 2017.



- Lefebvre, W. and Goosse, H.: Influence of the Southern Annular Mode on the sea ice-ocean system: the role of the thermal and mechanical forcing, *Ocean Science*, 1, 145-157, 2005.
- Lefebvre, W., Goosse, H., Timmermann, R., and Fichefet, T.: Influence of the Southern Annular Mode on the sea ice–ocean system, *Journal of Geophysical Research: Oceans* (1978–2012), 109, 2004.
- 350 Livezey, R. E., Vinnikov, K. Y., Timofeyeva, M. M., Tinker, R., and van den Dool, H. M.: Estimation and extrapolation of climate normals and climatic trends, *Journal of Applied Meteorology and Climatology*, 46, 1759-1776, 2007.
- Mahlstein, I., Gent, P. R., and Solomon, S.: Historical Antarctic mean sea ice area, sea ice trends, and winds in CMIP5 simulations, *Journal of Geophysical Research: Atmospheres*, 118, 5105-5110, 10.1002/jgrd.50443, 2013.
- Marshall, G. J.: Trends in the Southern Annular Mode from Observations and Reanalyses, *Journal of Climate*, 16, 4134-4143, 2003.
- 355 Matear, R. J., O’Kane, T. J., Risbey, J. S., and Chamberlain, M.: Sources of heterogeneous variability and trends in Antarctic sea-ice, *Nature Communications*, 6, 2015.
- Meehl, G. A., Arblaster, J. M., Chung, C. T., Holland, M. M., DuVivier, A., Thompson, L., Yang, D., and Bitz, C. M.: Sustained ocean changes contributed to sudden Antarctic sea ice retreat in late 2016, *Nature Communications*, 10, 1-9, 2019.
- Meier, W. N., Fetterer, F., Windnagel, A. K., and Stewart, J. S.: Near-Real-Time NOAA/NSIDC Climate Data Record of Passive Microwave Sea Ice Concentration, Version 2, NSIDC: National Snow and Ice Data Center [dataset], <https://doi.org/10.7265/tgam-yv28>, 2021a.
- 360 Meier, W. N., Fetterer, F., Windnagel, A. K., and Stewart, J. S.: NOAA/NSIDC Climate Data Record of Passive Microwave Sea Ice Concentration, Version 4, NSIDC: National Snow and Ice Data Center [dataset], <https://doi.org/10.7265/efmz-2t65>, 2021b.
- Mo, K. C. and Higgins, R. W.: The Pacific–South American Modes and Tropical Convection during the Southern Hemisphere Winter, *Monthly Weather Review*, 126, 1581-1596, 1998.
- 365 Mo, K. C. and Paegle, J. N.: The Pacific–South American modes and their downstream effects, *International Journal of Climatology*, 21, 1211-1229, 10.1002/joc.685, 2001.
- O’Kane, T. J., Risbey, J. S., Franzke, C., Horenko, I., and Monselesan, D. P.: Changes in the metastability of the midlatitude Southern Hemisphere circulation and the utility of nonstationary cluster analysis and split-flow blocking indices as diagnostic tools, *Journal of the atmospheric sciences*, 70, 824-842, 2013a.
- 370 O’Kane, T. J., Matear, R. J., Chamberlain, M. A., Risbey, J. S., Sloyan, B. M., and Horenko, I.: Decadal variability in an OGCM Southern Ocean: Intrinsic modes, forced modes and metastable states, *Ocean Modelling*, 69, 1-21, 2013b.
- Parkinson, C. L.: A 40-y record reveals gradual Antarctic sea ice increases followed by decreases at rates far exceeding the rates seen in the Arctic, *Proceedings of the National Academy of Sciences*, 116, 14414-14423, 2019.
- Parkinson, C. L. and Cavalieri, D. J.: Antarctic sea ice variability and trends, 1979–2010, *The Cryosphere*, 6, 871-880, 2012.
- 375 Peng, G., Meier, W. N., Scott, D., and Savoie, M.: A long-term and reproducible passive microwave sea ice concentration data record for climate studies and monitoring, *Earth System Science Data*, 5, 311-318, 2013.
- Raphael, M.: A zonal wave 3 index for the Southern Hemisphere, *Geophysical Research Letters*, 31, 2004.
- Raphael, M., Marshall, G., Turner, J., Fogt, R., Schneider, D., Dixon, D., Hosking, J., Jones, J., and Hobbs, W.: The Amundsen Sea Low: Variability, Change and Impact on Antarctic Climate, *Bulletin of the American Meteorological Society*, 2015.
- 380 Raphael, M. N. and Handcock, M. S.: A new record minimum for Antarctic sea ice, *Nature Reviews Earth & Environment*, 1-2, 2022.
- Raphael, M. N. and Hobbs, W.: The influence of the large-scale atmospheric circulation on Antarctic sea ice during ice advance and retreat seasons, *Geophysical Research Letters*, 41, 5037-5045, 10.1002/2014GL060365, 2014.
- Roach, L. A., Dörr, J., Holmes, C. R., Massonnet, F., Blockley, E. W., Notz, D., Rackow, T., Raphael, M. N., O’Farrell, S. P., and Bailey, D. A.: Antarctic sea ice area in CMIP6, *Geophysical Research Letters*, 47, e2019GL086729, 10.1029/2019GL086729, 2020.
- 385 Schlosser, E., Haumann, F. A., and Raphael, M. N.: Atmospheric influences on the anomalous 2016 Antarctic sea ice decay, *Cryosphere*, 12, 1103-1119, 2018.
- Schossler, V., Aquino, F. E., Reis, P. A., and Simões, J. C.: Antarctic atmospheric circulation anomalies and explosive cyclogenesis in the spring of 2016, *Theoretical and Applied Climatology*, 141, 537-549, 2020.
- Schroeter, S., Hobbs, W., and Bindoff, N. L.: Interactions between Antarctic sea ice and large-scale atmospheric modes in CMIP5 models, *The Cryosphere*, 11, 789, 10.5194/tc-11-789-2017, 2017.
- 390 Seviour, W., Codron, F., Doddridge, E. W., Ferreira, D., Gnanadesikan, A., Kelley, M., Kostov, Y., Marshall, J., Polvani, L., and Thomas, J.: The Southern Ocean sea surface temperature response to ozone depletion: a multimodel comparison, *Journal of Climate*, 32, 5107-5121, 2019.
- Shu, Q., Song, Z., and Qiao, F.: Assessment of sea ice simulations in the CMIP5 models, *The Cryosphere*, 9, 399-409, 2015.
- 395 Shu, Q., Wang, Q., Song, Z., Qiao, F., Zhao, J., Chu, M., and Li, X.: Assessment of sea ice extent in CMIP6 with comparison to observations and CMIP5, *Geophysical Research Letters*, 47, e2020GL087965, 10.1029/2020GL087965, 2020.
- Simmonds, I.: Comparing and contrasting the behaviour of Arctic and Antarctic sea ice over the 35 year period 1979-2013, *Annals of Glaciology*, 56, 18-28, 2015.
- 400 Stammerjohn, S. E., Martinson, D. G., Smith, R. C., Yuan, X., and Rind, D.: Trends in Antarctic annual sea ice retreat and advance and their relation to El Niño–Southern Oscillation and Southern Annular Mode variability, *Journal of Geophysical Research: Oceans*, 113, 10.1029/2007JC004269, 2008.



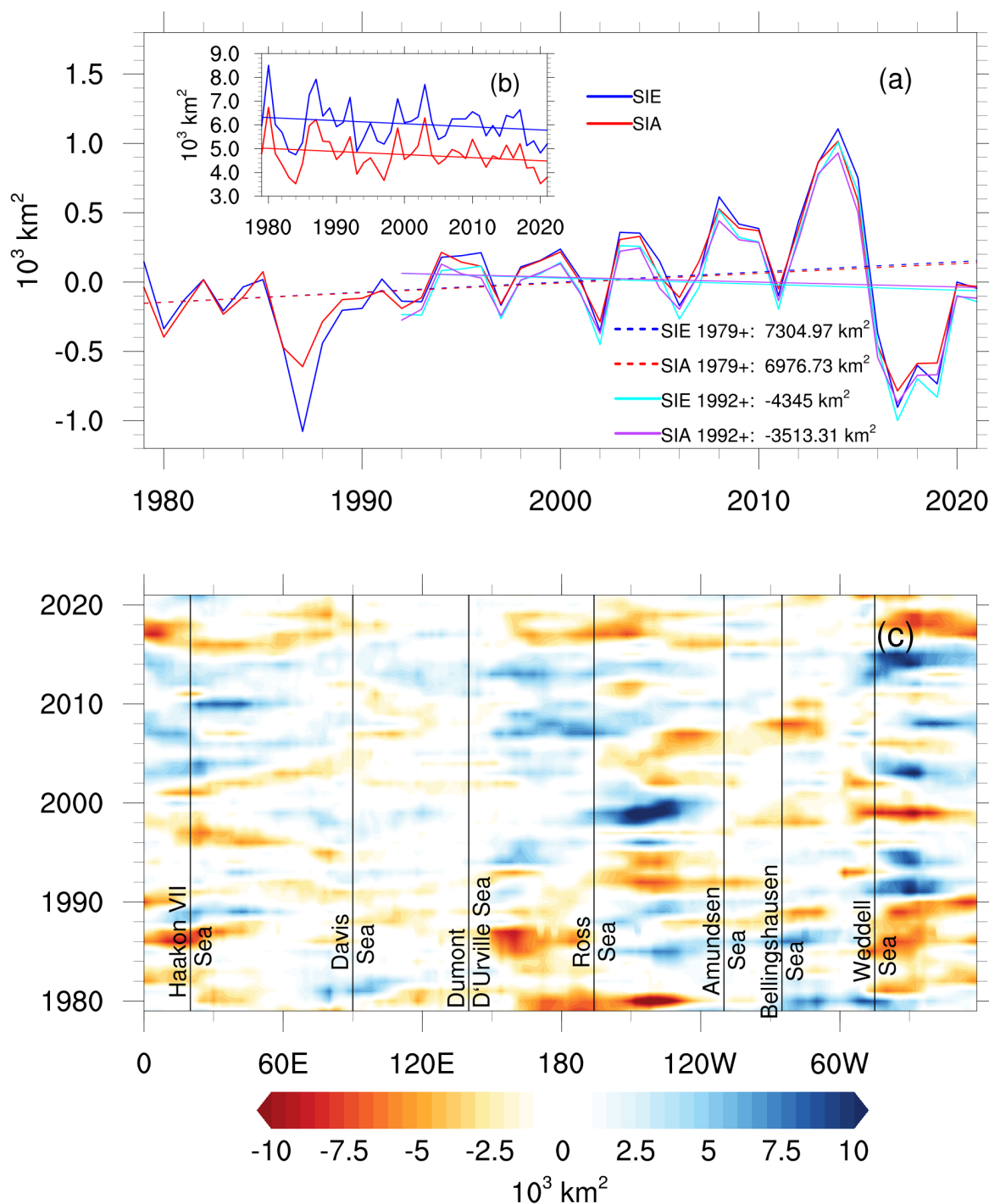
- Stuecker, M. F., Bitz, C. M., and Armour, K. C.: Conditions leading to the unprecedented low Antarctic sea ice extent during the 2016 austral spring season, *Geophysical Research Letters*, 44, 9008-9019, 2017.
- 405 Thompson, D. W. J. and Wallace, J. M.: Annular Modes in the Extratropical Circulation. Part I: Month-to-Month Variability, *Journal of Climate*, 13, 1000-1016, 10.1175/1520-0442(2000)013<1000:AMITEC>2.0.CO;2, 2000.
- Turner, J., Bracegirdle, T. J., Phillips, T., Marshall, G. J., and Scott Hosking, J.: An initial assessment of antarctic sea ice extent in the CMIP5 models, *Journal of Climate*, 26, 1473-1484, 10.1175/JCLI-D-12-00068.1, 2013a.
- Turner, J., Hosking, J. S., Bracegirdle, T. J., Marshall, G. J., and Phillips, T.: Recent changes in Antarctic sea ice, *Philosophical Transactions of the Royal Society A: Mathematical, Physical and Engineering Sciences*, 373, 20140163, 2015.
- 410 Turner, J., Phillips, T., Hosking, J. S., Marshall, G. J., and Orr, A.: The Amundsen Sea low, *International Journal of Climatology*, 33, 1818-1829, 10.1002/joc.3558, 2013b.
- Turner, J., Phillips, T., Marshall, G. J., Hosking, J. S., Pope, J. O., Bracegirdle, T. J., and Deb, P.: Unprecedented springtime retreat of Antarctic sea ice in 2016, *Geophysical Research Letters*, 44, 6868-6875, 2017.
- 415 Turney, C. S., Fogwill, C. J., Palmer, J. G., Van Sebille, E., Thomas, Z., McGlone, M., Richardson, S., Wilmshurst, J. M., Fenwick, P., and Zunz, V.: Tropical forcing of increased Southern Ocean climate variability revealed by a 140-year subantarctic temperature reconstruction, *Climate of the Past*, 13, 231-248, 2017.
- Verfaillie, D., Pelletier, C., Goosse, H., Jourdain, N. C., Bull, C., Dalaiden, Q., Favier, V., Fichefet, T., and Wille, J. D.: The circum-Antarctic ice-shelves respond to a more positive Southern Annular Mode with regionally varied melting, *Communications Earth & Environment*, 3, 1-12, 2022.
- 420 Wachter, P., Beck, C., Philipp, A., Höppner, K., and Jacobeit, J.: Spatiotemporal variability of the Southern Annular Mode and its influence on Antarctic surface temperatures, *Journal of Geophysical Research: Atmospheres*, 125, e2020JD033818, 2020.
- Wang, G., Hendon, H. H., Arblaster, J. M., Lim, E.-P., Abhik, S., and van Rensch, P.: Compounding tropical and stratospheric forcing of the record low Antarctic sea-ice in 2016, *Nature communications*, 10, 1-9, 2019.
- 425 Wang, J., Luo, H., Yang, Q., Liu, J., Yu, L., Shi, Q., and Han, B.: An Unprecedented Record Low Antarctic Sea-ice Extent during Austral Summer 2022, 2022.
- Zwally, H. J., Comiso, J. C., Parkinson, C. L., Campbell, W. J., and Carsey, F. D.: Antarctic sea ice, 1973-1976: Satellite passive-microwave observations, DTIC Document, 1983.



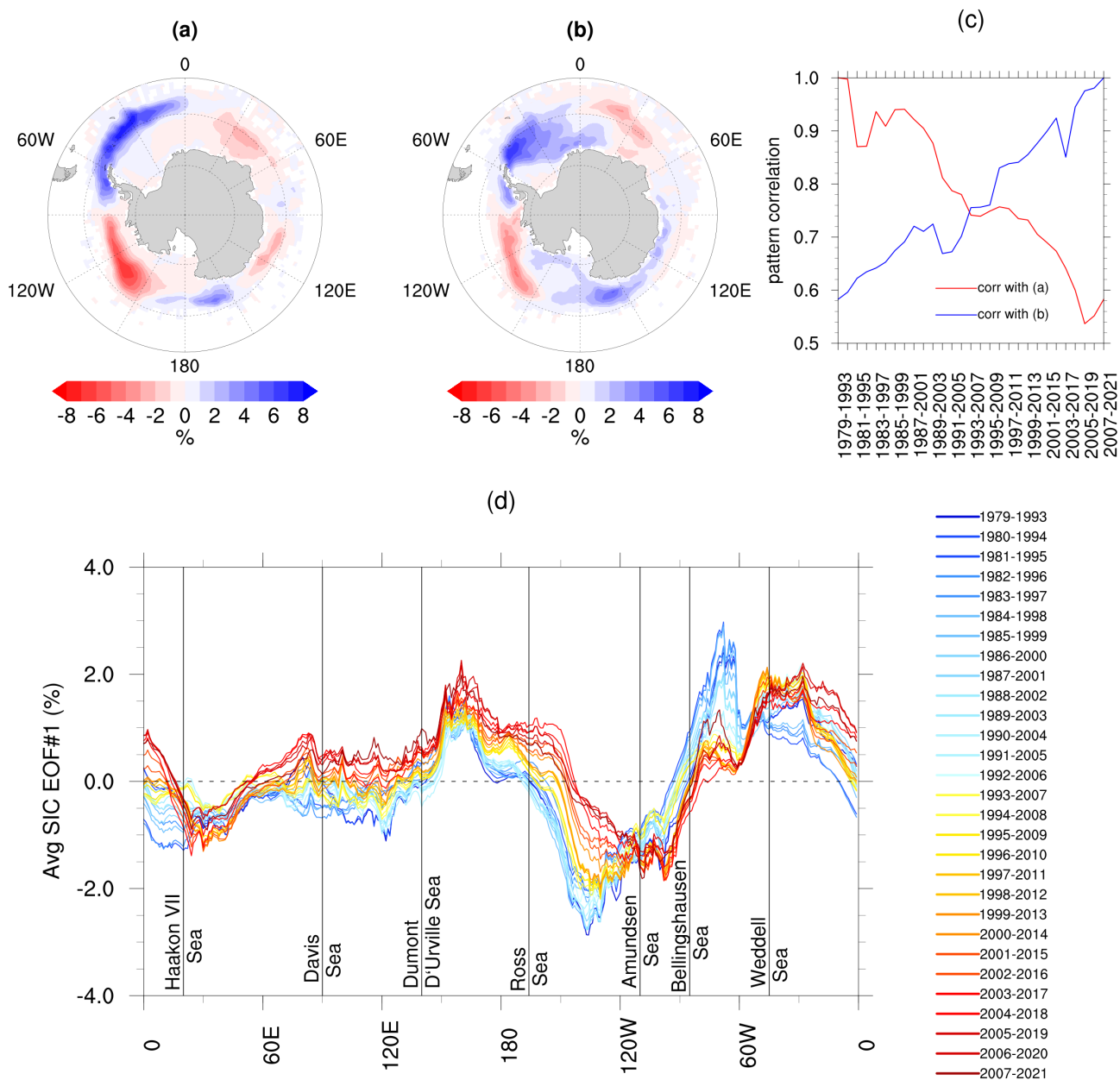
430

435

**Figure 1: Running 15-year SIA climatologies for (a) integrated circumpolar total SIA and SIE, (b-c) deviation of each 15-year climatology from the 1979-2021 climatologies of SIA and SIE, respectively, and (d-e) deviations of regional 15-yr annual mean SIA and SIE from 1979-2021 annual means. Lines are coloured from earliest (1979-1993, dark blue) to most recent (2007-2021, dark red) 15-yr samples. Vertical lines indicate approximate mid-point of each geographical location; zero deviation from long-term mean denoted by horizontal dotted line.**



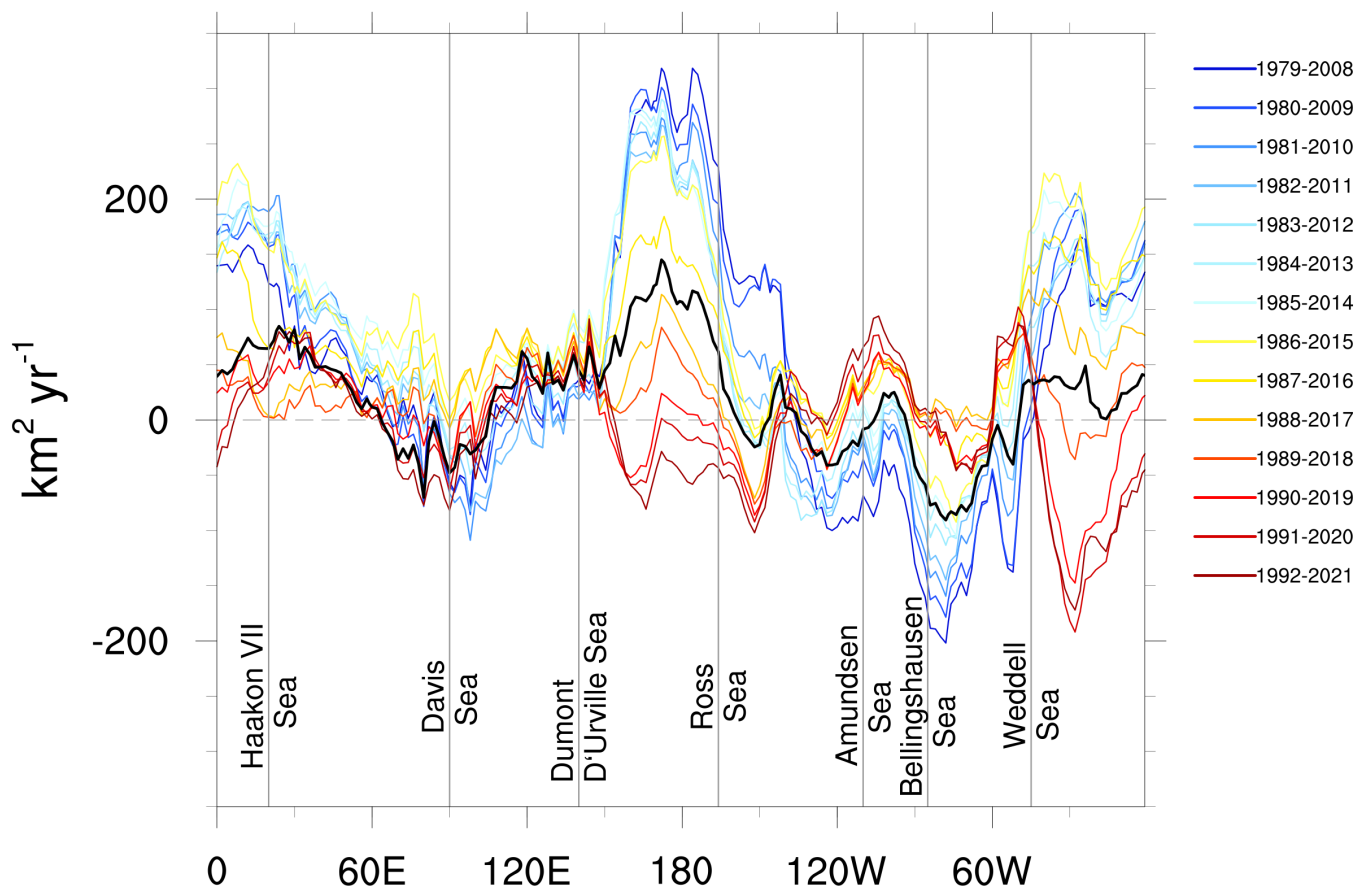
440 **Figure 2: (a) Annual average spatially-integrated anomalies of SIA and SIE for long-term satellite record duration (1979-2021) and most recent 30-yr period (1992-2021), (b) monthly average standard deviation of spatial anomalies from the 1979-2021 mean, and (c) annual average anomalies of SIA from the 1979-2021 climatology. Vertical lines in (c) indicate approximate mid-point of each geographical location.**



445

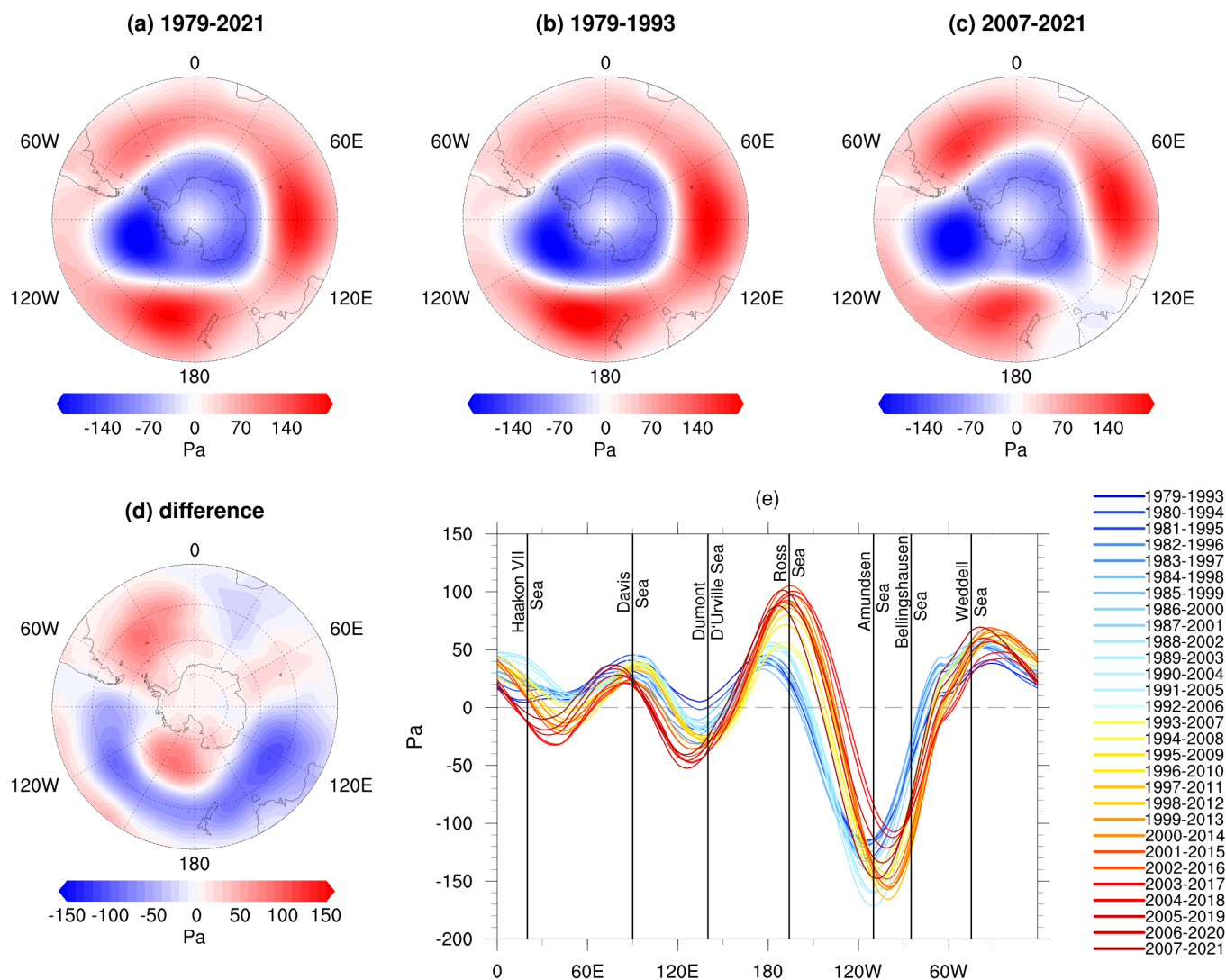
450

**Figure 3:** EOF1 of detrended SIC anomalies for (a) 1979-1993 and (b) 2007-2021, (c) pattern correlation of each 15-year sample with (a) and (b), and (d) average EOF1 by longitude for each 15-year sample. Lines are coloured from earliest (1979-1993, dark blue) to most recent (2007-2021, dark red) 15-year sample. Vertical grey lines indicate approximate mid-point of each geographical location depicted by vertical text.



455 **Figure 4: Running regressions of annual SIA anomalies from 30-year mean. Lines are coloured from earliest (1979-2008, dark blue) to most recent (1992-2021, dark red) 30-year sample. Thick black line indicates 1979-2021 annual average regression of SIA anomalies (i.e. long-term trend). Vertical grey lines indicate approximate mid-point of each geographical location depicted by vertical text.**

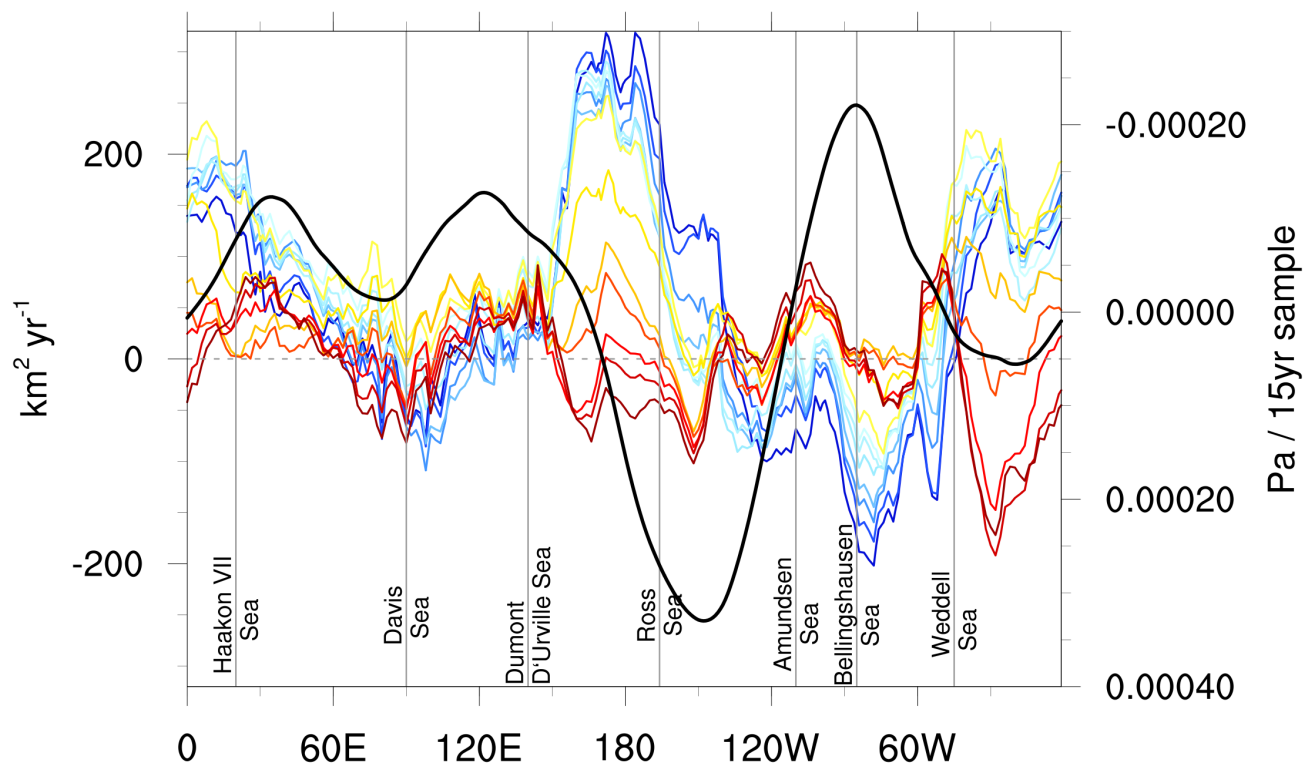




460

**Figure 5:** EOF1 of detrended SLP anomalies for (a) 1979-1993 and (b) 2007-2021, (c) difference between (a) and (b), and (d) average zonal anomaly of EOF1 between  $-70^{\circ}\text{S}$  and  $-55^{\circ}\text{S}$  for each 15-year sample. Lines are coloured from earliest (1979-1993, dark blue) to most recent (2007-2021, dark red) 15-year sample. Vertical lines indicate approximate mid-point of each geographical location depicted by vertical text.

465

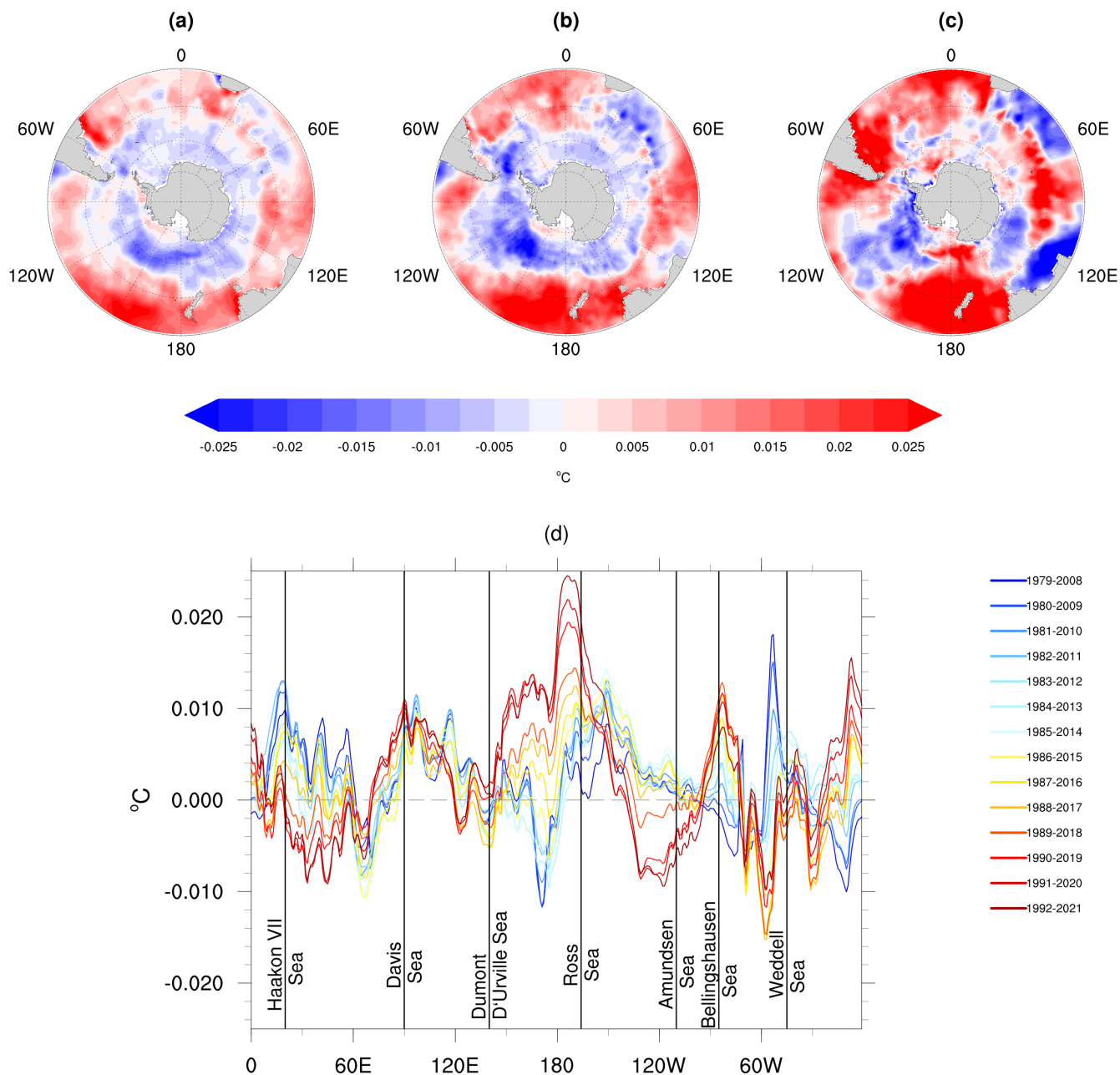


470

Figure 6: Gradient of (black line) 15yr samples of average -70°S to -55°S EOF1 zonal anomaly (Figure 5d), with 30-year annual SIA trends (as in Figure 4) by longitude. Sea ice regression lines are coloured from earliest (1979-2008, dark blue) to most recent (1992-2021, dark red) 30-year sample. Vertical grey lines indicate approximate mid-point of each geographical location depicted by vertical text.

475

480



485 **Figure 7: Annual average regression coefficients of Southern Ocean SST between: (a) 1979-2021; (b) 1992-2021; (c) 2007-2021; and (d) 30-year running samples averaged over the region north of the ice edge (-55°S to -40°S). Lines are coloured from earliest (1979-2008, dark blue) to most recent (1992-2021, dark red) 30-year SST sample. Vertical lines indicate approximate mid-point of each geographical location depicted by vertical text.**